A New 147–56 hPa Water Vapor Product from the UARS Microwave Limb Sounder.

W. G. Read, D. L. Wu, J. W. Waters, and H. C. Pumphrey

Jet Propulsion Laboratory, California Institute of Technology, Pasadena, CA.

Abstract. Measurements of H_2O in the tropopause region have been obtained by production of a new dataset from the Microwave Limb Sounder (MLS) on the Upper Atmosphere Research Satellite (UARS). A modified version of the retrieval scheme used to produce upper tropospheric humidity (UTH) from the MLS 203 GHz radiometer was applied to the MLS 183 GHz radiometer measurements to produce useful H_2O data at 147, 121, 100, 83, 68, and 56 hPa. These new data, for the first 18 months of the UARS mission when the MLS 183 GHz radiometer was operational, fill an important 'gap' around 100 hPa where previous MLS H_2O data were generally not useful. Characteristics of the new dataset are discussed and compared with National Oceanic and Atmospheric Administration (NOAA), Climate Monitoring and Diagnostics Laboratory (CMDL) frostpoint hygrometer and UARS Halogen Occultation Experiment (HALOE) measurements. *INDEX TERMS:* 3362 Meteorology and Atmospheric Dynamics: Stratosphere/troposphere interactions, 3314 Meteorology and Atmospheric Dynamics: Convective processes, 3374 Meteorology and Atmospheric Dynamics: Tropical meteorology.

1. Introduction

Progress toward understanding the processes that control atmospheric water vapor and its exchange between the troposphere and the stratosphere has been slow [*Kley et al.*, 2000]. Contributing to the difficulty is a lack of water vapor observations in the uppermost troposphere between 150 hPa (net zero radiative heating in the tropics) and the tropopause throughout the tropics. We describe here a new data set from the Microwave Limb Sounder (MLS) on board the Upper Atmosphere Research Satellite (UARS) that fill an important 'gap' around 100 hPa. The new data set is used to examine stratospheric dehydration [*Read et al., J. Geophys. Res.*, This issue].

The UARS [*Reber*, 1993] launched September 12, 1991 carries the MLS instrument [*Barath et al.*, 1993] that measures atmospheric limb thermal radiation with radiometers operating at 63, 183, and 203 GHz. A summary of MLS measurements and scientific results is given by *Waters et al.* [1999], and a summary of its data coverage and operations is in *Livesey et al.* [2003]. Previously there have been two distinct H_2O data products from MLS: (1) 'stratospheric H_2O' covering altitudes from 68 to 0.1 hPa with occasional measurements down to 100 hPa, hereafter referred to as V0104, the recommended data version for this product [*Pumphrey*, 1999] and (2) 'upper tropospheric humidity (UTH)', covering altitudes from 464 to 147 hPa and hereafter referred to as V4.9, its recommended data version [*Read et al.*, 2001]. The V0104 product is currently available at the Goddard Distributed Active Archive Center as MLS V6 H_2O. These products are distinct because stratospheric H_2O is retrieved exclusively from 183 GHz radiometer while UTH is retrieved exclusively from 203 GHz radiometer data. Connecting them has been problematic because V0104 is rarely useful at 100 hPa in the tropics and V4.9 sensitivity at 147 hPa is no better than $\sim$8 parts per million in volume (ppmv). Moreover, V4.9 has some undesirable artifacts at 147 hPa [*Read et al.*, 2001].

We have developed a new MLS H_2O dataset, hereafter referred to as 'V7.02 H_2O', to fill the gap around 100 hPa that exists in previous MLS H_2O datasets. V7.02 H_2O can be used with V4.9 and V0104 to give a continuous vertical profile from 464 to 0.1 hPa with 3–4 km vertical resolution. As with other MLS data products, useful measurements are made in the presence of cirrus (especially important near the tropical tropopause) and aerosol, with $\sim$1300 profiles obtained daily between 34°S–81°N or 81°S–34°N, depending on the UARS yaw state (which alternates 10 times per year). V7.02 H_2O data are available for most days from 19 September 1991 (shortly after launch) to 24 April 1993 (just before failure of the 183 GHz radiometer). The following sections discuss how the V7.02 H_2O data are produced and compare them with some other measurements.

2. UARS MLS V7.02 H_2O data

MLS V7.02 H_2O is produced by applying the strategy used for producing V4.9 UTH [*Read et al.*, 2001] to MLS channels 61 and 62 (on edge of the MLS 183 GHz H_2O band). Main features of this strategy are fitting to absolute radiance values rather than to spectral contrast as done for other MLS measurements, and characterization of the dry and moist continuum emission using measured radiances. Differences of V7.02 retrievals from V4.9 are: (1) H_2O is retrieved in volume mixing ratio (VMR) rather than relative humidity with respect to ice (%RHi), and (2) the moist continuum parameters of *Pardo et al.* [2001] are used.

The measured radiances in channels 61 and 62 are weighted sums of emission in the lower sideband near 183 GHz (relatively close to the strong H_2O line), and in the upper sideband near 186 GHz (where H_2O emission is much weaker). A spectrum observed by the MLS 183 GHz radiometer showing the two sidebands is given in *Lahoz et al.* [1996]. Figure 1 shows the radiance contribution to channels 61 and 62 for a specified amount of water as a function of its altitude (colored curve) and the field of view direction, tangent height (y-axis). The radiance contribution is the derivative of the radiance with respect to water vapor concentration in the specified layer (radiance Jacobian) times the H_2O concentration in the said layer. The third panel shows the radiance signal by sideband. The tangent altitude range where the radiance grows from near 0 to $\sim$ 100 K is the altitude range of the H_2O profile where that channel is most sensitive. As one can see, the 186 GHz sideband is good for measuring H_2O between 147–215 hPa. Note however, that the sensitivity drops rapidly when H_2O concentration exceeds $\sim$100 ppmv ($\sim$200 hPa, 12.5 km, in the tropics). This is evident in Figure 1 where the peak of the 261 hPa contribution is 5–8 times less than that for the lower pressure levels. The loss in sensitivity is a consequence of H_2O absorption between 215 and 261 hPa preventing the MLS observing H_2O at pressures higher than 215 hPa.

The 183 GHz sideband is good for measuring water vapor from 100 hPa and higher. Another aspect of the measurement system is its severe nonlinearity in the 186 GHz sideband where H_2O varies by a factor of ten or more. The profile in Figure 1 is representative of the tropics. At high latitudes, especially in winter where the tropopause is at a much lower altitude, the 186 GHz sideband will have better sensitivity to water vapor at lower altitudes than shown in Figure 1.

The radiance forward model requires absorption coefficient functions for both the dry continuum and moist contributions. The dry continuum arises mostly from the collision induced absorption between nitrogen and oxygen molecules

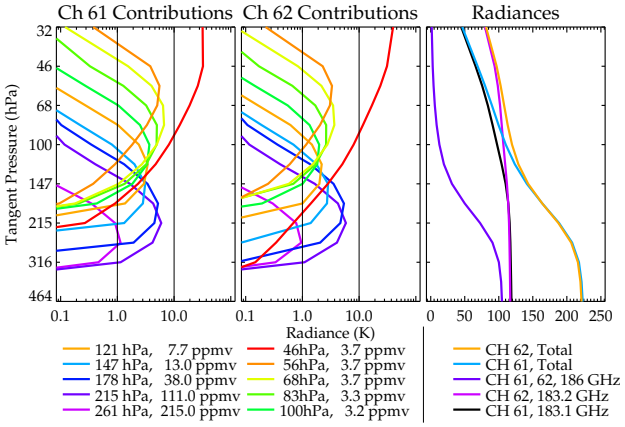

Figure 1. The two left panels show contributions to the radiances measured by MLS channels 61 and 62 respectively, as a function of observation path tangent pressure. The different colors indicate contributions from H_2O in layers at the different pressures as indicated. The radiance contribution is the radiance Jacobian times the H_2O concentration in the layer indicated by the color. The rightmost panel shows the sideband fraction weighted radiance signals at 183 GHz, and 186 GHz (same for both channels) and the double sideband signals for channels 61 and 62.

and wings of oxygen line emissions [*Liebe et al.*, 1993; *Pardo et al.*, 2001; *Borysow and Frommhold*, 1986; *Dagg et al.*, 1985, and, references cited therein]. The dry continuum was characterized by fitting parameters in the 186 GHz signal calculation. We needed to separate the 186 GHz contribution from the total signal. The center 5 channels, where the 183 GHz sideband is sensitive to water vapor at altitudes above 10 hPa, and temperature below, provide an opportunity to make this separation. Using several randomly selected days, the forward model using MLS retrieved H_2O and temperature are calculated for the 5 center 183 GHz channels. The computed signals are multiplied by the relative sideband response determined for MLS band 5 by *Pumphrey and Büehler* [2000] and differenced from the measured radiance. This gives the 186 GHz contribution (multiplied by its sideband fraction). This exercise produced an unrealistic negative radiance artifact between 50 and 20 hPa which could be tuned out with a -3% adjustment of the sideband fraction. Therefore we applied a -3% adjustment to the 183 GHz sideband fractions and used these modified values here and in subsequent data processing. The dry continuum function was determined using the 186 GHz radiance signal following the procedure described in *Read et al.* [2001]. The resulting dry continuum absorption coefficient

is $\alpha = 5.5 \times 10^{-9} p^2 (300/T)^4$ km^{-1}, where p is pressure in hPa, T is temperature in Kelvin, and the multiplicative constant and temperature exponent were fitted. This was used for both the 183 and 186 GHz sidebands. An independently derived wet function was not fitted because the absorption coefficient from the well characterized 183.3 GHz H_2O line [*Bauer et al.*, 1989; *Goyette and DeLucia*, 1990] accounts for 99.9% and 95.0% of the H_2O absorption coefficient at 183 and 186 GHz. The H_2O continuum measured by *Pardo et al.* [2001] was added to the H_2O line by line calculation.

Figure 1 also illustrates why using absolute radiances is, for the altitude region of interest here, superior to using spectral contrast for the H_2O measurement. It shows the radiance contribution from H_2O at ten separate altitudes (indicated by different colors) as a function of observation tangent pressure for MLS channels 61 and 62 used here. Spectral contrast is sensitive to differences in radiances measured by different spectral channels (e.g., MLS channels 62 and 61). Atmospheric spectral line widths at the low altitudes are large compared to widths of the UARS MLS bands, and the channel-to-channel differences become very small, making spectral contrast methods very sensitive to noise amplification. However, uncertainties in the absolute value of measured radiances — which are much larger than uncertainties in the spectral contrast — prevent the absolute radiance method from being applied to weak signals. The uncertainty in the absolute value of MLS radiances is $\sim$2 K, and one can see from Figure 1 that this should allow useful H_2O measurements between 215 hPa and 46 hPa from MLS channels 61 and 62. Note the 46 hPa coefficient shown in figure 1 includes all H_2O contributions from altitudes above 46 hPa. A description of the absolute radiance fitting procedure is given in *Read et al.* [2001]. A description of the spectral contrast fitting procedure is given by *Livesey et al.* [2003], and *Pumphrey* [1999].

The V7.02 H_2O vertical profile, like MLS V4.9 UTH, is modeled as piece-wise linear in logarithm of VMR as a function of atmospheric pressure, with breakpoints at 316, 261, 215, 178, 147, 121, 100, 83, 68, 56, and 46 hPa ($10^{(30-n)/12}$ where n is an integer from 0–10). The decision to have 12 breakpoints per decade change in pressure versus 6 per decade which is customary for UARS products improved 100 hPa H_2O performance in simulation tests and provided better profile sampling. The H_2O VMR is assumed constant at pressures higher than 316 hPa and lower than 46 hPa — altitude ranges where perhaps except for wintertime high latitudes, channels 61 and 62 are insensitive to H_2O and provide little information. Optimal estimation algorithms, as described by *Livesey et al.* [2003] for MLS V5 data, were used to retrieve the breakpoint values. The MLS V5 data provided the observation path tangent height and temperature for the V7.02 H_2O retrievals. At the heights of interest here, the V5 temperatures, are from the National Centers for Environmental Prediction (NCEP)/ Climate Prediction Center (CPC). The temperature is a NCEP/CPC global data assimilation system product that is provided on a 65$\times$65 polar stereographic grid.

The a priori H_2O values (uncertainties) used for V7.02 retrievals were 200(200) ppmv at 316 hPa, 120.0(150.0) ppmv at 261 hPa, 75(100) ppmv at 215 hPa, 40(60) ppmv at 178 hPa, 15(20) ppmv at 147 hPa, 10(10) ppmv at 121 hPa, and 5(5) ppmv at 100, 83, 68, 56, and 46 hPa. The large a priori uncertainties ensure insignificant impact of the a priori on the retrievals at altitudes of interest here. Radiance uncertainties used in the retrieval were (in brightness temperature units) 2 K for pressures less than 147 hPa, increasing linearly with log pressure to 5 K at 215 hPa, and 5K for pressures greater than 215 hPa. The forward model used a channel-center monochromatic calculation and measured antenna pattern [*Jarnot et al.*, 1996]. A yaw cycle artifact present in V4.9 [*Read et al.*, 2001] was removed in V7.02 H_2O by correcting the measured radiances for each day of processing according to the average 'space radiance' (measured each limb scan when the antenna is pointed above the region of atmospheric signal) for that day.

The V7.02 H_2O retrievals can have bias artifacts caused by limited vertical resolution and dynamic range of H_2O sensitivity. Vertical resolution is limited primarily by the 3.8 km width of the field-of-view at the tangent point. Sensitivity is limited to H_2O values less than $\sim$100 ppmv, above which both the MLS 183 and 186 GHz signals are optically thick. Based on National Oceanic and Atmospheric Administration (NOAA) Climate Monitoring and Diagnostics Laboratory (CMDL) frostpoint sounding data [http://www.cmdl.noaa.gov/ftpdata.html], and MLS V4.9 UTH [*Read et al.*, 2001] the 100 ppmv H_2O is near 200 hPa in the tropics, increasing to 350 hPa at high latitudes. Figure 2 shows what happens when large values and/or sharp kinks in the H_2O profile are introduced in a simulation retrieval. Test profile 1 uses a tropical temperature profile with 100% RHi up to 100 hPa, it has $>$100 ppmv H_2O at pressures $>$180 hPa. The retrieval for this profile severely underestimates H_2O at 316, and 261 hPa. H_2O at 215 hPa is 30% too low. The retrieved values at altitudes above 177 hPa agree with test profile values to within 15%. The 100 hPa H_2O is low by 0.6 ppmv. Test profile 2 shows what happens if H_2O has a large lapse rate change at 121 hPa. Inadequate vertical resolution causes the retrieved profile to smooth over the sharp kink leading to a severe high bias at 121 hPa. The rest of the profile at altitudes above 177 hPa are within 15%. The 100 hPa H_2O is low by 0.5 ppmv—about the same as profile 1. Profile 3 has half the H_2O of profile 1. The 215 hPa H_2O

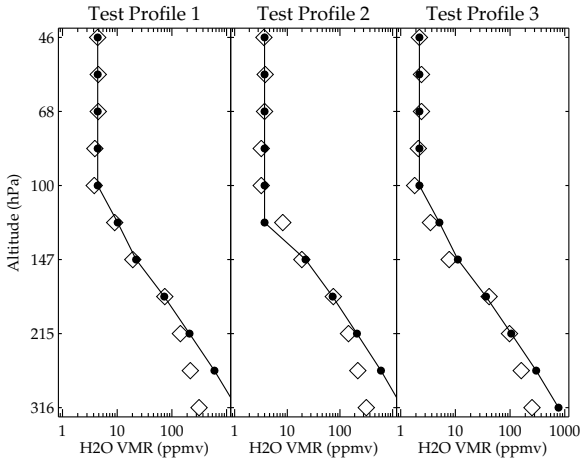

Figure 2. Simulation retrievals for three H_2O test profiles. The lines (with bullets at their breakpoints) are the test profile. Diamonds are retrievals of these profiles using the V7.02 algorithms. The profile 1 (left) is H_2O that is 100% relative humidity with respect to ice up to 100 hPa in the tropics. Profile 2 (center) is the same as on the left but with a low value kink introduced at 121 hPa. Profile 3 (right) has H_2O concentrations that are half that of profile 1.

is 105 ppmv and is retrieved well as are the stratospheric levels at altitudes above 100 hPa. The 147, 121, and 100 hPa have about the same biases as they did for profile 1 which are -3, -1.5, and -0.5 ppmv but because the profile is half as large, the % difference is double (30% for 147 and 121 hPa).

All available measurements between 19 September 1991 and 24 April 1993 were processed, with results stored in ASCII level 2 files in the same format as that used for UARS V4.9 and V5 UTH data [*Read et al.*, 2001]. These files contain profiles of H_2O in VMR and %RHi, and temperature as well as the radiance measurements, calculated radiances and the χ^2 of the fit. The %RHi is calculated from VMR and UARS MLS V5 temperature data (NCEP) using the Goff-Gratch function [*Read et al.*, 2001; *List*, 1951]. Temperature at the intermediate levels between the standard UARS levels are obtained from linear interpolation. Discontinuities in the retrieved H_2O values are observed for a few isolated days and after 15 April 1993 which may be related to the 183 GHz radiometer failure which occurred a short time later. Data shown in this paper are restricted to the 3 October 1991 to 15 April 1993 period with a few spurious days removed. Table 1 lists estimates of retrieved single-profile accuracy, precision, and vertical resolution (full width at half maximum of the averaging kernel). The estimated accuracies are based on mapping the 2–5 K radiance uncertainties into H_2O. These errors are assumed to include uncertainties in

Table 1. Estimated Precision, Accuracy, and Resolution for MLS V7.02 H_2O

Level, hPa	Precision,[a] ppmv	Accuracy,[b] ppmv	Resolution,[c] km
56	0.09	1.5	3.5
68	0.11	1.2	3.1
83	0.07	1.6	4.0
100	0.10	1.3	4.0
121	0.20	3.1	4.1
147	0.36	5.3	4.1
178[d]	0.18	12.	5.2
215[d]	1.8	24.	4.2

[a]Precision: minimum observed variability in a five day 5° zonal mean.

[b]Accuracy: based on 2–5 K uncertainties on the radiances.

[c]Resolution is half width of the averaging kernel.

[d]These levels should only be used when V7.02 215 hPa $H_2O <$ 15 ppmv. The V4.9 215 hPa H_2O is recommended when V7.02 215 hPa $H_2O > 15$ ppmv.

tangent pressure, temperature, and the dry absorption coefficient function as was done for UTH [*Read et al.*, 2001]. An upper limit on precision is obtained from the standard deviation of the data about the zonal mean from 5 consecutive days, choosing the 5° latitude bin where the standard deviation is minimum. The minimum variability at all levels is seen at high latitudes in its summer season.

Clouds in the field-of-view appear to have a minimal impact upon the V7.02 H_2O retrievals. Very thick clouds often cause the radiance fit χ^2 to exceed 30 and all V7.02 data having these values should be rejected. Only 0.6% of the data have $\chi^2 > 30$. The long wavelengths used by the MLS instrument make cloud detection difficult except for the thickest clouds having large diameter particles (> 50 μm) [*D. Wu et al.*, submitted to *J. Atmos. Sci.*, 2003]. A cloud retrieval scheme has been developed for MLS based on the 203 GHz window channel [*D. Wu et al.*, submitted to *J. Atmos. Sci.*, 2003]. The cloud retrieval computes a quantity called 'cloud radiance' which is the difference between an atmosphere having 110 %RHi and the measured radiance. Clouds are indicated when the cloud radiance is ≥ 3 K. Figure 3 shows a scatter plot comparison between cloud radiance and retrieved %RHi (derived from a VMR retrieval using its coincident NCEP temperature), an average %RHi as a function of cloud radiance, and the percentage of data having a cloud radiance greater than indicated on the x-axis at 147, 121, and 100 hPa. Only data between 25°S and 25°N are considered because this cloud detection method works best up to the tropopause. Testing cloud impacts at 100 hPa lim-

its this technique to the tropics. A direct comparison to the MLS cloud product is possible because MLS cloud and H_2O data are coincident, and can isolate the impacts to the thickest clouds. Cloud radiances < 3 K are proportional to H_2O, with larger negative values indicating low %RHi. Therefore we expect a monotonically increasing trend of %RHi with cloud radiance up to 3 K. Cloud radiances > 3 K indicate that the atmosphere is cloudy and saturated; therefore, retrieved %RHi should be constant. Figure 3 indeed shows a clear break in the monotonically increasing trend in %RHi occurs near 3 K with only slight increases with increasing cloud radiance except at the highest cloud radiances, (>20 K). It is noteworthy that the break occurs at different relative humidities for the different pressures and are less than 100 %RHi. Likely explanations for this are biases in the NCEP temperature data used to compute the relative humidity and biases in the MLS H_2O, both are altitude dependent. For example, we will show later that the MLS V7.02 100 hPa H_2O is 20% drier than other correlative data and it is also known that the NCEP temperatures used here are 4 K higher than representative radiosonde observations [*Randel et al.*, 2000] in the tropical tropopause region. Compensating for these two effects would move the breakpoint from 40 to 90 %RHi. The %RHi where the breaks occur at the other levels are consistent with the likely biases in the V7.02 MLS H_2O and NCEP temperatures. Also shown on the plot are the raw averages of the data versus a calculation where the cloudy points are set to the %RHi of the 3 K value as a cloud clearing scheme. The averages show very little overall cloud impact. Also noteworthy is that <1% of the data (cloud radiances > 20 K at 121 and 100 hPa and 30 K at 147 hPa) appears to be adversely affected by clouds. One needs to be cautious when looking at individual profiles (or making one-day maps) where little or no averaging is done. Such points can be detected because they will appear as spikes (high values with no orbital track correlation) in the data and can be rejected. The V7.02 data presented in the paper do not use any cloud screening techniques except for rejecting retrievals having $\chi^2 > 30$.

The V7.02 retrievals produce better H_2O at pressures of 147, 100, and 68 hPa than previous versions of MLS data, but V4.9 still has the best MLS H_2O at pressures above 147 hPa and V0104 the best at pressures at and below 46 hPa. A future goal is to produce a single H_2O dataset from MLS that covers the troposphere to the mesosphere. To do so will require will require laboratory measurements of the dry and moist continuum [work in progress, F. DeLucia, 2004], and temperature data that is more accurate in the tropopause region than the NCEP analyses used here [*Randel et al.*, 2000].

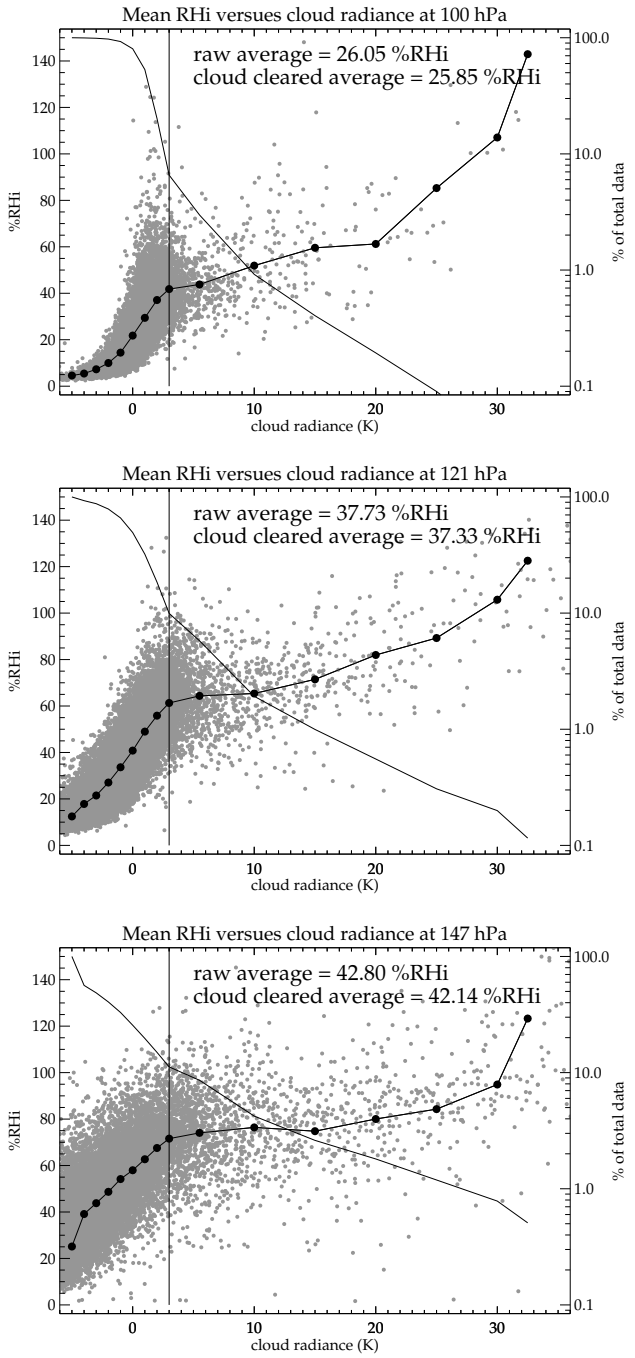

Figure 3. Scatterplot of cloud radiance versus V7.02 H_2O in %RHi at (top) 100 hPa, (center) 121 hPa, and (bottom) 147 hPa. The line with bullets is average %RHi as a function of cloud radiance. The plain line is (right y-axes) percentage of measurements having cloud radiances equal or greater than that given by the x-axis. The data are from January to March, 1992, 25°S–25°N. Cloud radiance > 3 K indicates high probability of a cloud in the MLS field-of-view.

3. Comparisons with Other Measurements

We compare the V7.02 H_2O with MLS V4.9, MLS V0104, NOAA CMDL balloon-based frostpoint hygrometer (FPH) and UARS HALogen Occultation Experiment (HALOE) measurements. The emphasis of these comparisons is how well the MLS V7.02 H_2O follows seasonal variations because in a companion paper [*Read et al., J. Geophys. Res.*, This issue] we look at the seasonal evolution of H_2O and compare it to model predictions near the tropical tropopause.

Comparisons with MLS V4.9 and V0104 data show how well the V7.02 profiles overlap the previously-validated MLS data — an essential consideration for combining the three datasets in scientific studies. Figure 4 shows a zonal mean comparison among these three datasets. The left panel shows only V4.9 and V0104. The region between 147 hPa and 100 hPa is not sampled by either dataset and is missing in Figure 4. The right panel shows the V7.02 dataset inserted between either 215 or 147 hPa and 56 hPa inclusive. We use the V7.02 215 hPa H_2O when it measures less than 15 ppmv (at 215 hPa). Although the V7.02 retrieval retrieval extends down to 316 hPa, we do not use the V7.02 at pressures where $H_2O > 15$ ppmv because, the V4.9 data are better. The morphology of the 316 and 215 hPa H_2O V7.02 daily mapped fields (not shown) agree very well with V4.9, but the V7.02 is 40% dryer at 215 hPa in the tropics and mid-latitudes.

Noteworthy is that the tropical V7.02 is 40% drier than V4.9 at 147 hPa, which deserves some discussion. The V4.9 retrieval is done in %RHi. The relative humidity unit when combined with the radiometric insensitivity of the submillimeter wave emissions from cirrus allowed the determination of the dry and moist continuum from in-orbit data. In the case of the moist continuum, a distinct maximum value of radiance measurements as a function of height could be identified which is representative of the atmosphere being in 100 %RHi. The conversion of relative humidity to concentration which is necessary for the radiative transfer calculation is strongly temperature dependent. Therefore the measured in-orbit continuum functions which are used in the radiance forward model will be impacted by the temperature dataset used. Because the in-orbit derived continuum functions include the temperature biases, these biases will be compensated for in the retrieved H_2O provided that humidity is expressed in relative humidity units. Therefore, from a retrieval perspective, the V4.9 humidity in %RHi is approximately independent of the temperature data set used in its retrieval. However, the effect of temperature errors appear when V4.9 %RHi is converted to volume mixing ratio as has been done here. The V7.02 H_2O is retrieved in volume mixing ratio so that temperature errors on retrieved VMR have a small effect. The V4.9 147 hPa %RHi were compared to a small number of coincident FPH and to a larger number of coincident Vaisala radiosonde humidity measurements. These comparisons show that the MLS V4.9 147 hPa %RHi was 8% higher than the FPH and 11% lower than the radiosonde, indicating acceptable agreement [*Read et al.*, 2001]. The 147 hPa comparison shows the V4.9 zonal mean using NCEP temperatures for the conversion. Had we used European Centre for Medium range Weather Forecasts (ECMWF) reanalysis temperatures for the conversion which are 2 K cooler [*Pawson and Fiorino*, 1999], the zonal mean in the tropics would be 25% drier than shown. This adjustment would make the V7.02 147 hPa H_2O 25% drier (3.5 ppmv) than V4.9. Although temperature bias doesn't account for all the difference, it is within the accuracy of the respective datasets [*Read et al.*, 2001]. The mid-latitude notch and yaw cycle artifacts in 147 hPa V4.9 data [*Read et al.*, 2001] are not present in V7.02.

The V0104 retrieved H_2O profile is an optimal estimate that combines MLS radiance measurements and a climatological H_2O mostly derived from several years of HALOE and SAGE II measurements [*Pumphrey*, 1999; *Russell III et al.*, 1993; *Rind et al.*, 1993]. At 100 hPa, the lowest altitude retrieved by the V0104 algorithm, H_2O is sometimes mostly the climatological input. When this is the case the uncertainty is made negative, indicating that MLS provides less than half the total information in the retrieved value. The tropical V0104 100 hPa H_2O is strongly influenced by climatology, whereas at mid-high latitudes, its measurement is mostly from MLS. The 100 hPa H_2O from V0104 shown in Figure 4 incorporates all its retrieved values including those influenced mostly by climatology. The V7.02 data are 10–20% drier 100 hPa, and 7% wetter at 68 hPa than V0104. There is a minor (relative to the estimated accuracy) oscillation in the vertical profile at 147(low), 121 (high), and 100 hPa (low) which can be seen at high latitudes where the H_2O profile gradient is small when the three datasets are joined.

Figure 5 shows a comparison of MLS V7.02, HALOE V19 corrected for its known dry bias [*Kley et al.*, 2000], and CMDL FPH soundings over Boulder, Colorado. The Boulder data set are balloon flights between 1990 and 1999 [data provided by NOAA/CMDL]. The FPH is accurate to 10% with excellent vertical resolution [*Oltmans*, 1985]. The HALOE V19 H_2O compares favorably with several independent measurement techniques *Kley et al.* [2000]. Comparisons show that the HALOE V19 H_2O has a dry bias ranging from 20% at 120 hPa to 5% at 60 hPa and lower. Therefore, we correct the HALOE data for these biases by reducing the 121, 100, 83, 68 and 56 hPa levels by 20%, 10%, 10%, 10%, and 5%, respectively. Such corrections have been applied

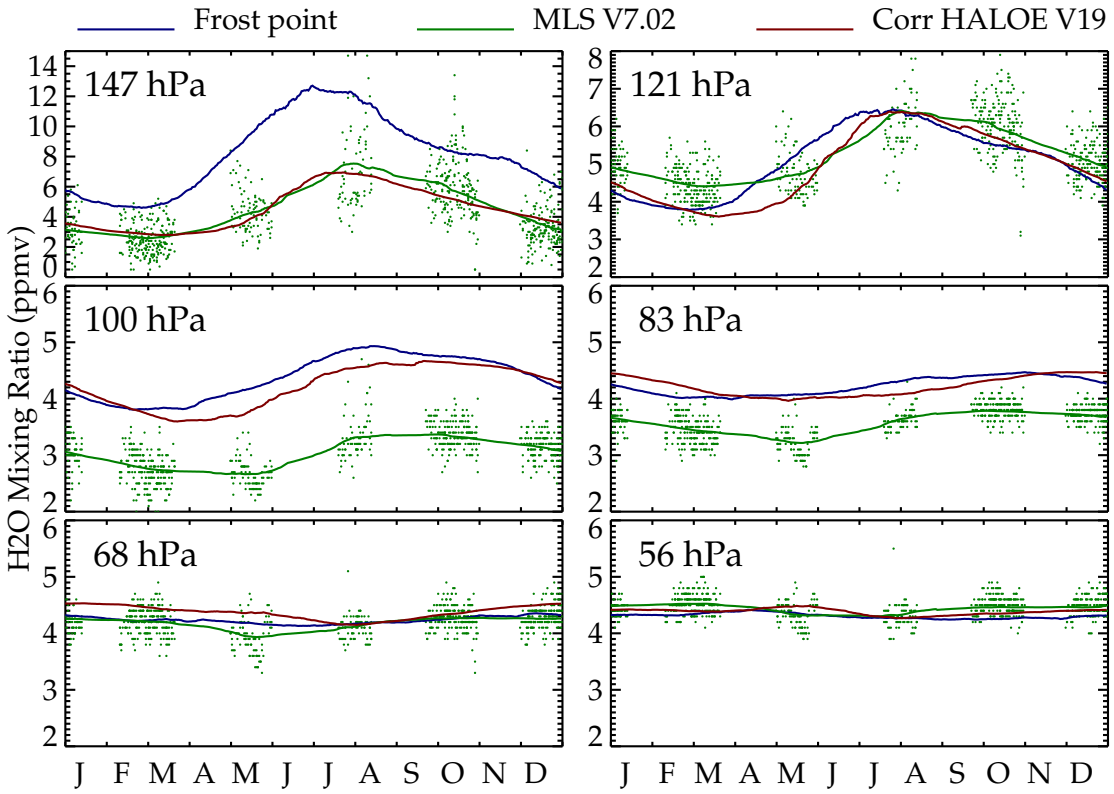

Figure 5. A comparison of the multi year seasonal cycle of H_2O over Boulder, Colorado. CMDL frostpoint hygrometer (1990–1999) is blue, corrected HALOE V19 (1992–2003, see text) is red, and MLS V7.02 (Oct. 1991–Apr. 1993) is green. Individual MLS measurements are shown as green points.

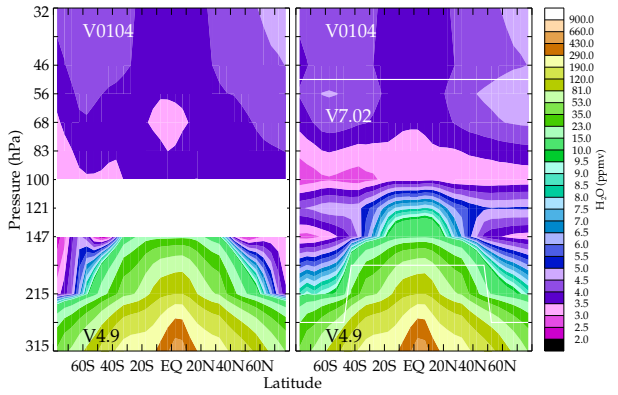

Figure 4. Zonal mean of water vapor versus pressure using MLS data taken in 1992. The left panel is the V4.9 and V0104 datasets. The blank region is where H_2O is not sampled by either dataset. The right panel shows the H_2O obtained from overlaying the V7.02 data between 147 and 56 hPa on the combined V4.9, and V0104 data. White lines on the right panel indicate the altitude ranges of the respective dataset used to produce the figure.

in other studies [*Randel et al.*, 2001]. HALOE V19 is also too dry at 147 hPa, but it does not behave in a uniform way therefore no correction has been applied to that level. All HALOE data from 1992 to 2003 and between 245°E–265°E, longitude, and 37°N–43°N, latitude is used. Most of the data was cloud screened according to *Hervig and McHugh* [1999]. Also shown is the MLS V7.02 H_2O over the same longitude and latitude range as HALOE but only from Oct. 1991 to April 1993, the mission lifetime of the 183 GHz radiometer. The mean seasonal cycle for all three data sets are derived from a two dimensional smoothing algorithm (30 days by 1.3 km) [*Zeng and Levy*, 1995] which grids the data by day-of-year and pressure. Figure 5 shows the individual MLS V7.02 data which show the monthly data gaps caused by UARS yaw maneuvers.

Agreement between the corrected HALOE V19 and the FPH is excellent between 100 and 56 hPa. Although MLS V7.02 has a significant dry bias between 147 and 83 hPa, it captures the seasonal cycle quite well except at 121 hPa where the MLS data underestimate the amplitude and show a 1 month delay in summertime moistening. HALOE which gets the amplitude accurately also shows a similar delay. MLS V7.02 and HALOE V19 show excellent agreement at 147 hPa, but both are 44% drier than the FPH. The average biases between the FPH and MLS V7.02 are: 2.9%, -31%, -16%, -1.5% and 2.8% at 121, 100, 83, 68, and 56 hPa respectively.

Table 2. Average of 26 CMDL frostpoint hygrometer profile measurements taken over the central equatorial Pacific ocean compared to an average of all MLS V7.02 profiles taken in March 1993 between 170°E–205°E longitude and 5°S–5°N latitude.

Level, hPa	MLS, ppmv	Hygrometer, ppmv	Diff,[a] ppmv	% Diff,[b] %
56	3.7	3.5	0.2	6.7
68	3.6	3.1	0.5	14.5
83	2.9	2.9	0.0	2.0
100	2.8	3.6	−0.8	−22.9
121	7.3	7.6	−0.3	−4.0
147	13.0	18.8	−5.8	−30.9

[a] MLS - Hygrometer.

[b] 100×(MLS - Hygrometer)/Hygrometer.

Table 2 shows a comparison between an average of 26 CMDL FPH soundings taken over the equatorial central Pacific in March 1993 (Central Equatorial Pacific Ocean Experiment, CEPEX [http://www-c4.ucsd.edu/c4publications/cepex_report.html]) and MLS V7.02 in March 1993 between 170°E–205°E, longitude, and 5°S–5°N, latitude. As with the Boulder, Co. comparisons, MLS V7.02 is significantly drier than the FPH at 147 hPa and 100 hPa.

To gain a global perspective regarding the quality of the MLS V7.02 H_2O, we look at comparisons with the HALOE V19 H_2O. The HALOE data have been corrected for their known dry biases at 121, 100 and 83 hPa with cloud contaminated H_2O removed. Figure 6 shows the seasonal cycle of the zonal H_2O from HALOE V19 (1992–2003) and MLS V7.02 on four levels between 147 and 83 hPa. These levels are inside the tropical tropopause layer (TTL). As with the FPH, MLS V7.02 is drier than HALOE at 100 and 83 hPa; however, the general features are in good agreement. Most notably, both datasets show the northward displacement of the moisture minimum and maximum at 100 hPa [*Randel et al.*, 2001]. The MLS data also show horizontal transport from the tropics towards the higher latitudes but MLS shows a strip of locally higher values near January–March centered at 15°S not evident in the HALOE data. This strip may be an artifact of poorer vertical resolution in the MLS data where the 121 hPa level is zonally high. MLS V7.02 is wetter than HALOE V19 at 121 and 147 hPa. Both HALOE V19 and MLS V7.02 show latitudinal tracking of maximum H_2O seasonally following the sun with a 1–2 month lag; however, the HALOE V19 shows evidence for horizontal trans-

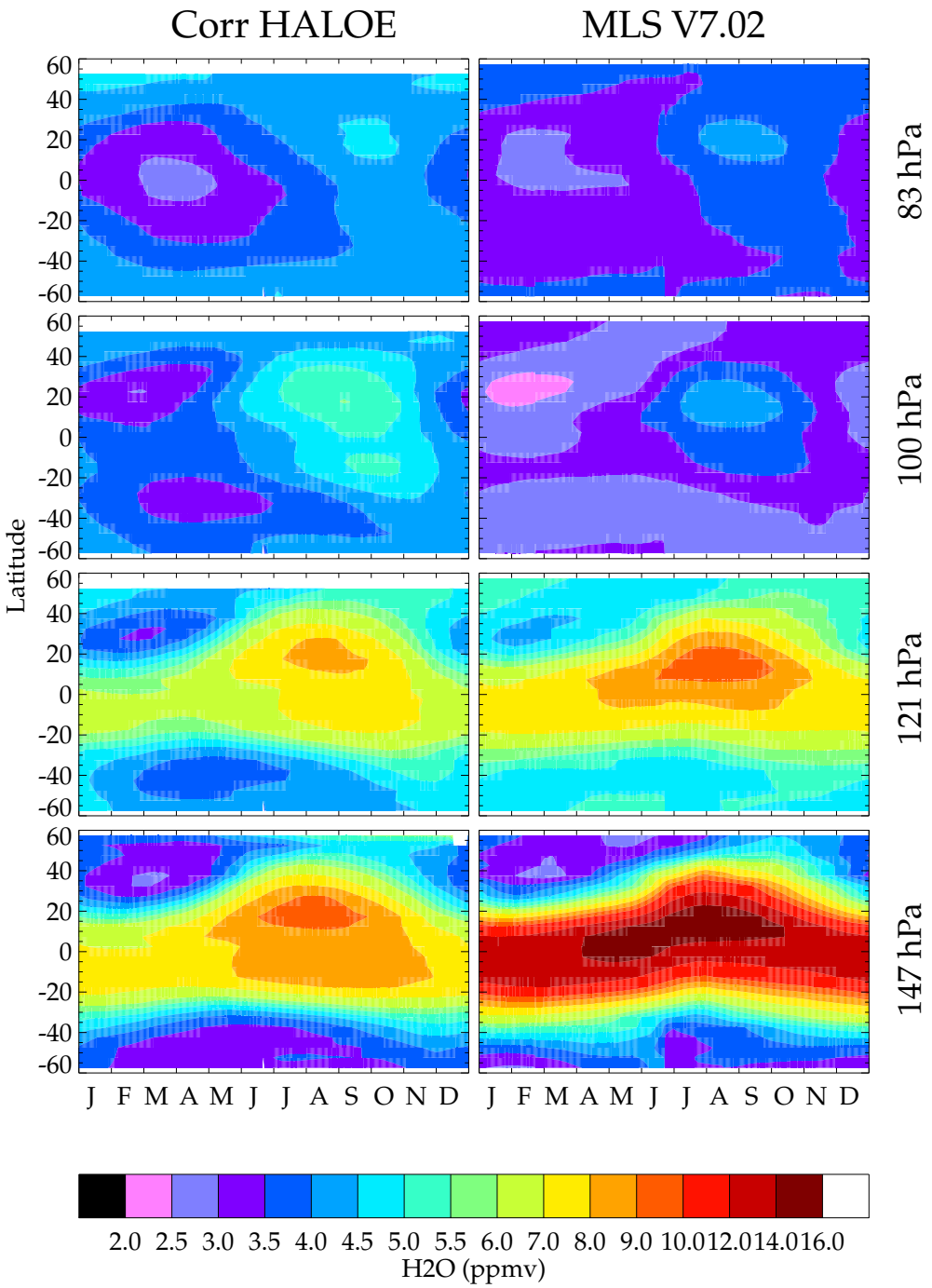

Figure 6. A climatology of zonal means by month and pressure for corrected HALOE V19 (1992–2003) (left panels) and MLS V7.02 (Oct. 1991–Apr. 2003) (right panels).

port of H_2O at 121 and 147 hPa like that seen at 100 hPa during the northern hemisphere summer. The MLS V7.02 only shows this weakly at 121 hPa. These differences are hard to understand and probably related to limitations associated with the HALOE and MLS measurement systems. MLS is minimally affected by clouds and therefore does not have a clear-sky sampling bias but has poorer vertical resolution. HALOE has better vertical resolution (2 km) but cannot measure H_2O in clouds. At 147 hPa, O_2 is a strong contaminating species in the HALOE H_2O measurement and is responsible for causing a large dry bias [*Kley et al.*, 2000].

Figure 7 shows the zonal/height seasonal cycle amplitude and phase differences between MLS V7.02 and corrected HALOE V19. The data used to produce Figure 6 were fit to a periodic function $Z = M + A\sin(2\pi(d+D)/365)$, where Z is the measurement (Figure 6) which is a function of day of year and pressure, M is the annual zonal mean, A is the seasonal cycle amplitude, d is the day of year of the measurement, and D is the phase of the seasonal cycle. Parameters M, A, and D are fitted. The top panel shows the percent difference (100*(MLS - HALOE)/HALOE) in M, the middle panel shows the relative percent difference (A/M) and the bottom panel shows the difference in D in months. MLS V7.02 seasonal amplitude is over 50% wetter than HALOE V19 at 147 hPa in the tropics. MLS is 20% wetter than HALOE at 121 hPa with minor latitude variation except towards higher northern latitudes where the bias drops under 10%. The 100 hPa shows MLS having a 25% dry bias with weak latitude dependence. At 83, 68, and 56 hPa, MLS on average differs from HALOE by -12%, -2%, 1% respectively.

The MLS V7.02 relative amplitude of the seasonal cycle compares quite favorably with HALOE especially in the tropics. The only notable exceptions are 147 and 121 hPa levels in the extratropics and mid latitudes where MLS is 10% larger and -10% smaller respectively.

The phase difference plot shows the results of the fit only where the estimated phase uncertainty for both MLS and HALOE is less than one month. Large estimated phase uncertainties occur when the seasonal cycle amplitude is weak or non-existent. MLS and HALOE show large phase differences in the tropics at 147 and 121 hPa and is easily seen in Figure 6. MLS H_2O maximum follows the seasonal solar cycle at 147 and 121 hPa whereas the maximum HALOE H_2O occurs in September–October throughout the tropics. This leads to the large phase differences seen by MLS and HALOE as shown in Figure 7. For example at 15°S, the MLS H_2O maximum occurs in February whereas for HALOE it is in August. MLS and HALOE phase differences agree within one month for the levels between 100 and 56 hPa. Since the MLS data only encompass 1.5 years versus 11 years for HALOE these differences could be a consequence of interannual variability. Due to heavy aerosol contamination from the Mt. Pinatubo eruption which prevented reliable HALOE retrievals near and below the tropopause, there is less than 1 year of overlap between the MLS and HALOE measurements, preventing further investigation of the impact interannual variability on these comparisons.

4. Conclusions

Water vapor with better quality than previously available from MLS at 147, 121, 100, 83, 68, and 56 hPa has been successfully obtained with the V7.02 algorithm. Cloud impacts are small with $< 1\%$ of the data being rejected due to poor fit quality or whose values are adversely influenced by ice. The V7.02 H_2O can be joined to the MLS V4.9 UTH and the V0104 stratospheric H_2O data, providing a vertical profile from 464 to 0.0046 hPa for most days when both the MLS 183 and 203 GHz radiometers were operational — between 19 September 1991 and 25 April 1993.

The comparisons done here show that the three MLS H_2O datasets can be joined, using V4.9 from 464–215 hPa, V7.02 from 147–56 hPa, and V0104 from 46–0.0046 hPa. The V7.02 147 hPa is 25–30% dry relative to central Pacific CMDL FPH and tropical MLS V4.9. The yaw cycle and mid-latitude notch artifacts in the V4.9 147 hPa H_2O have been eliminated in V7.02. The 121 hPa is within 5% of CMDL FPH in the central Pacific and Boulder, Colorado but shows variable agreement with corrected HALOE V19. MLS is 20% more moist in the tropics reducing to 5% at mid latitudes. At 100 hPa the CMDL and corrected HALOE indicate that MLS is 20–30% and too dry. A 15% dry bias at 100 hPa is also produced in simulations indicating that this is an artifact of the MLS V7.02 measurement system. The HALOE and CMDL FPH show that MLS 83 hPa is slightly dry ($< 10\%$) in the tropics increasing to 15% at mid latitudes. The lower pressure surfaces, 68 and 56 hPa appear to be slightly moist ($< 5\%$) compared to corrected HALOE. The relative amplitude of the seasonal cycle compares well with HALOE at pressures less than 121 hPa. At 121 hPa, the MLS underestimates the relative seasonal amplitude at mid-latitudes by as much as 10%—a result consistent with a CMDL FPH comparison over Boulder. MLS shows a stronger seasonal variation than HALOE at 147 hPa in mid-latitudes. The seasonal phase comparison compares well between MLS and corrected HALOE except in the tropics between 147 and 121 hPa where large differences exist. The MLS phase is consistent with maximum H_2O tracking the seasons whereas HALOE suggests that maximum H_2O is dominated by horizontal transport during the Northern Hemisphere summer moist period.

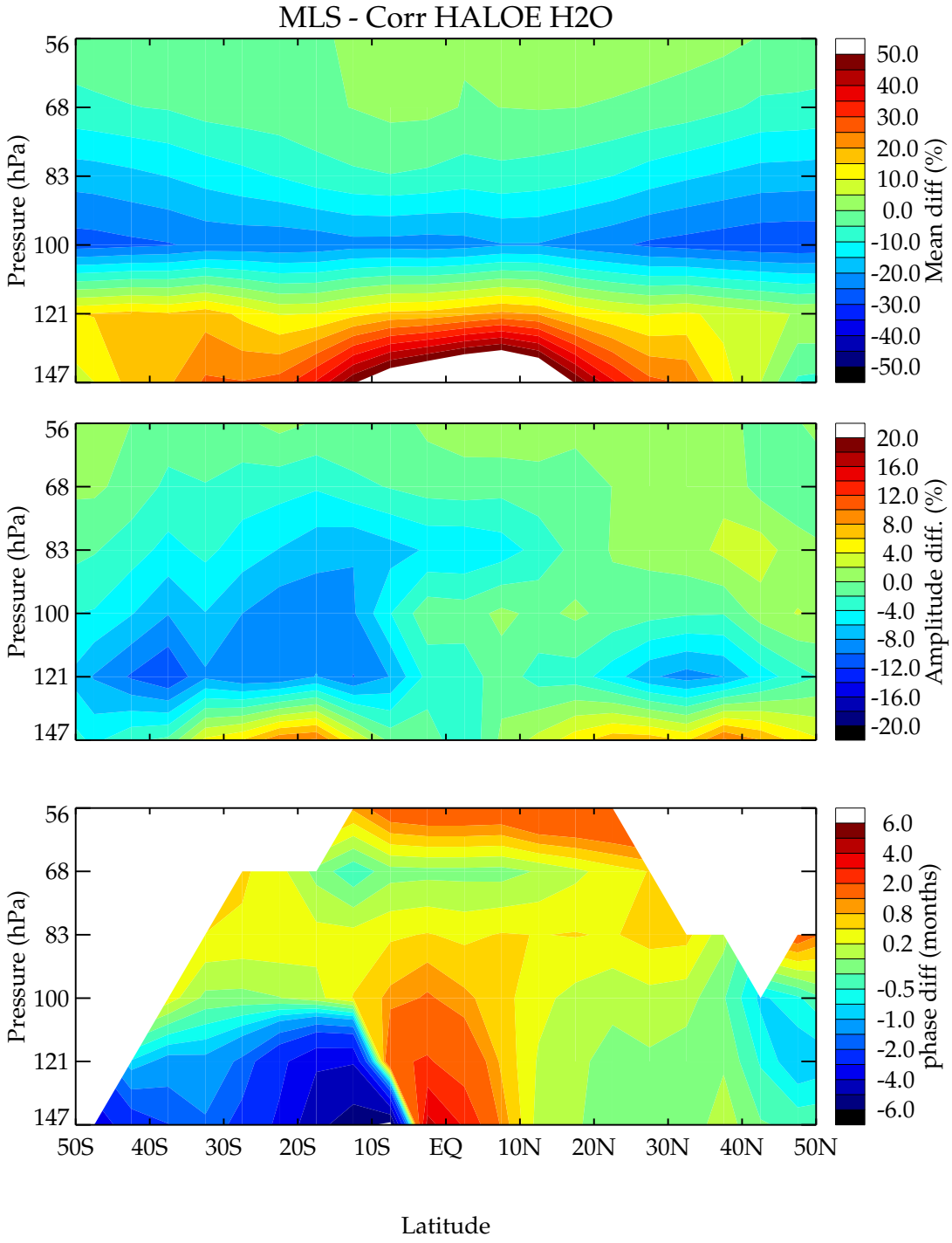

Figure 7. Difference in the zonal H_2O seasonal cycle amplitude and phase between MLS V7.02 (Oct.1991–Apr. 1993) and corrected HALOE V19 (1992–2003). The percent difference in the annual mean (top), percent difference in the relative amplitude (middle) and the phase difference (bottom) in months are shown.

Data usage recommendations for the V7.02 data are as follows:

- Use V7.02 between 147 and 56 hPa. V7.02 can be used down to 215 hPa when its $H_2O < 15$ppmv, otherwise use H_2O from V4.9.
- Reject any data having a $\chi^2 > 30$.
- Increase the MLS 147 hPa H_2O value and uncertainty by 30%.
- Increase the MLS 100 hPa H_2O value and uncertainty by 20%.

The corrections are aimed at minimizing the biases in the tropics, at higher latitudes, the biases are slightly larger. The accuracies and precisions shown in Table 1 for H_2O at 147 and 100 hPa should be increased by 30 and 20% respectively.

An improved MLS will be on the Earth Observing System's (EOS) Aura satellite to be launched in 2004 with an operational lifetime of 5 years or more. Unlike UARS MLS which was not designed for measurement of tropospheric and lower stratospheric H_2O, EOS MLS is designed to measure H_2O throughout the upper troposphere, stratosphere and mesosphere. The expected EOS MLS measurement precision for individual H_2O profiles retrieved at 6 levels per decade change in pressure (2.7 km) is 0.1–0.15 ppmv with a vertical resolution of 2.8 km in the TTL region. For H_2O profiles retrieved at 12 levels per decade (1.4 km), the precision is 2–3 ppmv with a vertical resolution of 2.1 km in the TTL. The successful retrieval of H_2O in the TTL from the UARS MLS lays the groundwork for obtaining a better data product from EOS MLS.

Acknowledgments. We thank two anonymous referees for their recommendations. We thank N. Livesey and M. Filipiak for providing the precision versus resolution data for the EOS MLS. This work was part of an effort at developing algorithms for retrieving H_2O in the TTL from measurements by EOS MLS to be launched in 2004 on the Aura satellite, and we thank Dr. M.R. Schoeberl, Aura Project Scientist, for encouraging and supporting our efforts in this area. The research described here done at the Jet Propulsion Laboratory, California Institute of Technology, was under contract with the National Aeronautics and Space Administration.

References

Barath, F. T., et al., The Upper Atmosphere Research Satellite Microwave Limb Sounder Instrument, *J. Geophys. Res.*, *98*, 10,751–10,762, 1993.

Bauer, A., M. Godon, M. Khedder, and J. M. Hartmann, Temperature and perturber dependences of water vapor line-broadening experiments at 183 GHz; calculations below 1000 GHz, *J. Quant. Spectrosc. Radiat. Transfer*, *41*, 49–54, 1989.

Borysow, A., and L. Frommhold, Collision-induced rototranslational absorption spectra of N_2–N_2 pairs for temperatures from 50 to 300 K, *Astrophys. J.*, *311*, 1043–1057, 1986.

Dagg, I. R., A. Anderson, S. Yan, W. Smith, and L. A. A. Read, Collision-induced absorption in nitrogen at low temperatures, *Can. J. Phys.*, *63*, 625–631, 1985.

Goyette, T. M., and F. C. DeLucia, The pressure broadening of the $3_{12} \rightarrow 2_{20}$ transition of water between 80 K and 600 K, *J. Mol. Spectrosc.*, *143*, 346–358, 1990.

Hervig, M. E., and M. J. McHugh, Cirrus detection using HALOE measurements, *Geophys. Res. Lett.*, *26*, 719–722, 1999.

Jarnot, R. F., R. E. Cofield, J. W. Waters, D. A. Flower, and G. E. Peckham, Calibration of the Microwave Limb Sounder on the Upper Atmosphere Research Satellite, *J. Geophys. Res.*, *101*, 9957–9982, 1996.

Kley, D., J. M. Russell III, and C. Phillips, SPARC assessment of upper tropospheric and stratospheric water vapour, *SPARC Report No. 2 WCRP-113*, WMO/ICSU/IOC, CNRS, Verrières le Buisson, 2000.

Lahoz, W. A., et al., Data validation of 183 GHz UARS MLS H_2O measurements, *J. Geophys. Res.*, *101*, 9957–9982, 1996.

Liebe, H. J., G. A. Hufford, and M. G. Cotton, Propagation modeling of moist air and suspended water/ice particles at frequencies below 1000 Ghz, in *52nd Specialists' Meeting of the Electromagnetic Wave Propagation Panel*, Adv. Group for Aerosp. Res. and Dev., Palma De Mallorca, Spain, 1993.

List, R. J., Smithsonian meteorological tables, *Smithson. Misc. Collect. 114*, Smithson. Inst., Washington, D. C., 1951.

Livesey, N. J., W. G. Read, L. Froidevaux, J. W. Waters, H. C. Pumphrey, D. L. Wu, M. L. Santee, Z. Shippony, and R. F. Jarnot, The UARS Microwave Limb Sounder version 5 dataset: Theory, characterization and validation, *J. Geophys. Res.*, *108*, 4378, doi:10.1029/2002JD002273, 2003.

Russell III, J. M., et al., The Halogen Occultation Experiment, *J. Geophys. Res.*, *98*, 10,777–10,798, 1993.

Oltmans, S., Measurements of water vapor in the stratosphere with a frost point hygrometer, in *Proceedings of the 1985 International Symposium on Moisture and Humidty*, pp. 251–258, Measurement and Control in Science and Industry, Instrum. Soc. of Am., Washington, D.C., 1985.

Pardo, J. R., E. Serabyn, and J. Cernicharo, Submillimeter atmospheric transmission measurements on Mauna Kea during extremely dry El Niño conditions: Implications for broadband opacity contributions, *J. Quant. Spectrosc. Radiat. Transfer*, *68*, 419–433, 2001.

Pawson, S., and M. Fiorino, A comparison of reanalyses in the tropical stratosphere. Part 3: inclusion of the pre-satellite data era, *Climate Dynamics*, *14*, 241–250, 1999.

Pumphrey, H. C., Validation of a new prototype water vapor retrieval for the UARS Microwave Limb Sounder, *J. Geophys. Res.*, *104*, 9399–9412, 1999.

Pumphrey, H. C., and S. Büehler, Instrumental and spectral parameters: Their effect on and measurement by microwave limb sounding of the atmosphere, *J. Quant. Spectrosc. Radiat. Transfer*, *64*, 421–437, 2000.

Randel, W. J., F. Wu, and D. J. Gaffen, Interannual variability of the tropical tropopause derived from radiosonde data and NCEP reanalyses, *J. Geophys. Res.*, *105*, 15,509–15,523, 2000.

Randel, W. J., F. Wu, A. Gettelman, J. M. R. III, J. M. Zawodny, and S. J. Oltmans, Seasonal variation of water vapor in the lower stratosphere observed in Halogen Occultation Experiment data, *J. Geophys. Res.*, *106*, 14,313–14,325, 2001.

Read, W. G., et al., UARS MLS upper tropospheric humidity measurement: Method and validation, *J. Geophys. Res.*, *106*, 32,207–32,258, 2001.

Reber, C. A., The Upper Atmosphere Research Satellite, *Geophys. Res. Lett.*, *20*, 1215–1218, 1993.

Rind, D., E.-W. Chiou, W. Chu, S. Oltmans, J. Lerner, J. Larsen, M. P. McCormick, and L. McMaster, Overview of the Stratospheric Aerosol and Gas Experiment II water vapor observations: Method, validation, and data characteristics, *J. Geophys. Res.*, *98*, 4835–4856, 1993.

Waters, J. W., et al., The UARS and EOS Microwave Limb Sounder experiments, *J. Atmos. Sci.*, *56*, 194–218, 1999.

Zeng, L., and G. Levy, Space and time aliasing structure in monthly mean polar-orbiting satellite data, *J. Geophys. Res.*, *100*, 5133–5142, 1995.

W. G. Read, D. L. Wu, J. W. Waters, Jet Propulsion Laboratory, Mail Stop 183-701, 4800 Oak Grove Drive, Pasadena, CA., 91109, USA. (bill@mls.jpl.nasa.gov; dwu@mls.jpl.nasa.gov; joe@mls.jpl.nasa.gov)

H. C. Pumphrey, Department of Meteorology, University of Edinburgh, James Clerk Maxwell Building, King's Buildings, Mayfield Road, Edinburgh, EH9, 3JZ, Scotland, U.K. (H.C.Pumphrey@ed.ac.uk)

October 18, 2002; revised Month day, year; accepted Month day, year.